Heliyon 5 (2019) e01731

Contents lists available at ScienceDirect

Heliyon

journal homepage: www.heliyon.com

Preparation of magnetic chitosan using local iron sand for mercury removal

Rahmi *, Fathurrahmi, Lelifajri, Fitri PurnamaWati

Chemistry Department, Universitas Syiah Kuala, Banda Aceh, Indonesia

ARTICLE INFO

Keywords:
Materials chemistry
Physical chemistry
Analytical chemistry

ABSTRACT

Preparation of magnetic chitosan for mercury removal from polluted water had been conducted. Magnetic particles (Fe_3O_4) were isolated from local iron sand to provide magnetic properties of chitosan. Glutaraldehyde was used as crosslinking agent of chitosan. The obtained magnetic chitosan was characterized by using FTIR, TGA, DSC, XRD, and SEM. Adsorption experiments were conducted with various contact time, pH and initial concentration of mercury. The results showed glutaraldehyde and Fe_3O_4 decreased crystallinity of chitosan. Low crystallinity of polymer is favorable for adsorption due to the high accessibility of adsorbate to reach active sites of adsorbent. FTIR and SEM confirmed the formation of magnetic chitosan. Based on correlation coefficient (R^2) values, the adsorption mercury by magnetic chitosan fitted with Langmuir and Freundlich isotherm models.

1. Introduction

Mercury is considered to be one of the most harmful metals found in the environment [1, 2]. It can threaten the health of people, fish, and wildlife everywhere. The disastrous consequences of its bioaccumulation (nervous system disorders, chromosomal aberrations, intellectual deterioration, etc.) are well known. Some materials had been used for mercury removal from polluted water such as sulfurized fibrous silicates [3], quartz and gibbsite [4], and sugi wood carbonized [5].

The formation of a coordination complex compound with metal ions is a good way to remove metal ions from a water solution. If a polymer molecule contains some functional groups such as amine, amide, and/or hydroxyl having one or more electron donor atoms such as N and O, it can adsorb metal ions by forming coordination compounds with them. Chitosan is a polymer that has the above stated properties, thus it is suitable to be used as an adsorbent for metal ions.

Chitosan has been reported in many works as a good adsorbent of heavy metal ions due to its biodegradability, availability, and low cost [6, 7]. However, the use of pure chitosan has some disadvantages due to its poor physical and chemical properties such as low mechanical properties and high solubility in acid solution. In order to reduce the disadvantages of chitosan, some modifications had been conducted [8, 9, 10, 11]. Zhou [12] reported that crosslinking could improve stability of chitosan in acid solution. Some researchers had reported chitosan modification by using Fe_3O_4 with the purpose to obtained magnetic chitosan [13, 14]. Magnetic chitosan is easily separated from water by using permanent magnet. Most of Fe_3O_4 used was commercial products or was produced by chemical precipitation. It is known that iron sand contains Fe_3O_4, whereas the iron sand is largely available in Aceh, Indonesia. Therefore in this work, we used Fe_3O_4 isolated from local iron sand in order to provide magnetic properties of chitosan and glutaraldehyde as a crosslinking agent in order to improve chitosan stability in acid solution.

Preparation of magnetic chitosan was performed with several content variations of chitosan, glutaraldehyde and Fe_3O_4. Magnetic chitosan obtained was then characterized by using FTIR, TGA, DSC, XRD and SEM. It was applied as an adsorbent of mercury in polluted water. Adsorption experiments were conducted with several contact time, pH and initial concentration of mercury. Mercury concentration was determined by using Atomic Adsorption Spectroscopy (AAS).

2. Materials and methods

2.1. Materials

Iron sand was obtained from Syiah Kuala beach, Aceh, Indonesia. Polluted water was collected from traditional gold mining area at Manggamat, Aceh, Indonesia. Chitosan was purchased from Tokyo Chemical Industry Co., Ltd. Japan (obtained from shrimp shell where deacetylation degree was 75.0–85.0%). All other chemicals were analytical grade and used as received without further purification.

2.2. Instrumentation

FTIR spectra of materials were detected by Shimadzu FTIR-Prestige

* Corresponding author.
E-mail address: rahmi@fmipa.unsyiah.ac.id (Rahmi).

https://doi.org/10.1016/j.heliyon.2019.e01731
Received 1 January 2019; Received in revised form 17 March 2019; Accepted 10 May 2019

21 Series Fourier Transform Infrared Spectrometer. Spectral scanning was acquired in a wave number ranged from 4500 to 400 cm^{-1}. XRD patterns were obtained with the Shimadzu XRD-700 Series X-Ray Diffractometer operating at 40kV and 30mA producing $Cu_{K\alpha}$ with λ = 0.154 nm in the range of 2θ = 10–80° using a step size of 0.02°/min. Micrographs were obtained with JSM-6510A/JSM-6510LA (Analytical/Analytical low vacuum SEM). SEM images were obtained at 100, 500 and 30,000x magnifications. Thermogravimetric analysis (TGA) was conducted using Shimadzu DTG-60 Serial No.C30564800501TK simultaneous DTA-TG. The experiments were performed with 5 mg of sample under nitrogen atmosphere flowing at a rate of 20 mL/min. The heating rate was 40 °C/min. DSC analysis was done by Shimadzu DSC-60 series Differential Scanning Calorimeter under air atmosphere. Heating rate and sample mass were similar to TGA analysis. Mercury ion concentrations were determined by using Shimadzu AA-6300 Atomic Absorption Spectrophotometer (AAS).

2.3. Fe_3O_4 isolation from iron sand

Iron sand (15 g) was added to beaker glass containing 100 mL HCl 12 M and stirred at 70 °C for 30 min. The solution was then filtered using a filter paper to separate undissolved particles. NH_4OH solution was dropped into the mixture under stirring at 70 °C for 30 min until the black precipitate was obtained. Permanent magnet was placed under the beaker glass with the purpose to extract Fe_3O_4 precipitated earlier than Fe_2O_3. The obtained black precipitate (Fe_3O_4) was dried in an oven at 70 °C overnight.

2.4. Preparation of magnetic chitosan

Preparation of magnetic chitosanwas conducted according to procedure reported by Udoetok [15] with some modifications. Where chitosan (0.35 g) was dissolved in 20 mL acetic acid (2%) and stirred for 2 h to form chitosan solution. Glutaraldehyde was added to chitosan solution and stirred for 2 h Fe_3O_4 particles (0.5 g) were added to crosslinked chitosan solution and stirred for 2 h. Dope solution was added to a syringe and dropwise into NaOH solution (3 M). The magnetic chitosan formed in NaOH solution was filtered and washed several times until neutral pH reached. The magnetic chitosan was dried in oven overnight at 40 °C.

2.5. Adsorption experiments

Magnetic chitosan (0.1 g) was placed in Erlenmeyer flask containing 10 mL Hg(II) solution with initial concentration of 30 ppm. The solution was shaken at 150 rpm for 80 min. After adsorption, magnetic chitosan was separated from solution by using permanent magnet. The final concentration of Hg(II) was determined by using AAS. The adsorption capacity (Q) was calculated using Eq. (1).

$$Q = \frac{(C_i - C_e)V}{W} \quad (1)$$

where C_i is initial concentration of Hg(II) and C_e is the concentration of Hg(II) at equilibrium. W is the weight of adsorbent and V is the volume of Hg(II) solution.

3. Results and discussion

3.1. FTIR

FTIR spectroscopy analysis was performed to study functional groups contained in the materials and to confirm the interaction between components. The FTIR spectra of chitosan, magnetic chitosan without and with crosslinking were shown in Fig. 1.

Fig. 1(a) showed FTIR spectrum of chitosan. It confirmed the presence of saturated hydrocarbons in the structure of chitosan. Band of $–NH_2$ stretching vibration occurred at wave number 3427.51 cm^{-1}. Bands at wave numbers 2856.58 and 2922.16 cm^{-1} showed bending vibration of –CH aliphatic and $–CH_2$ vibration, respectively. Stretching vibration of amide I was observed at wave number 1633.71 cm^{-1} [16]. Similar bands were also found in FTIR spectrum of magnetic chitosan without crosslinking (Fig. 1(b)). New band was found at wave number of 580.57 cm^{-1} that described the vibration of Fe–O [17, 18]. FTIR result indicated the presence of typical functional groups of Fe_3O_4. Fig. 1c showed FTIR spectrum of magnetic chitosan with crosslinking. Compared with FTIR spectrum of chitosan, absorption band at wave number 1633.71 cm^{-1}

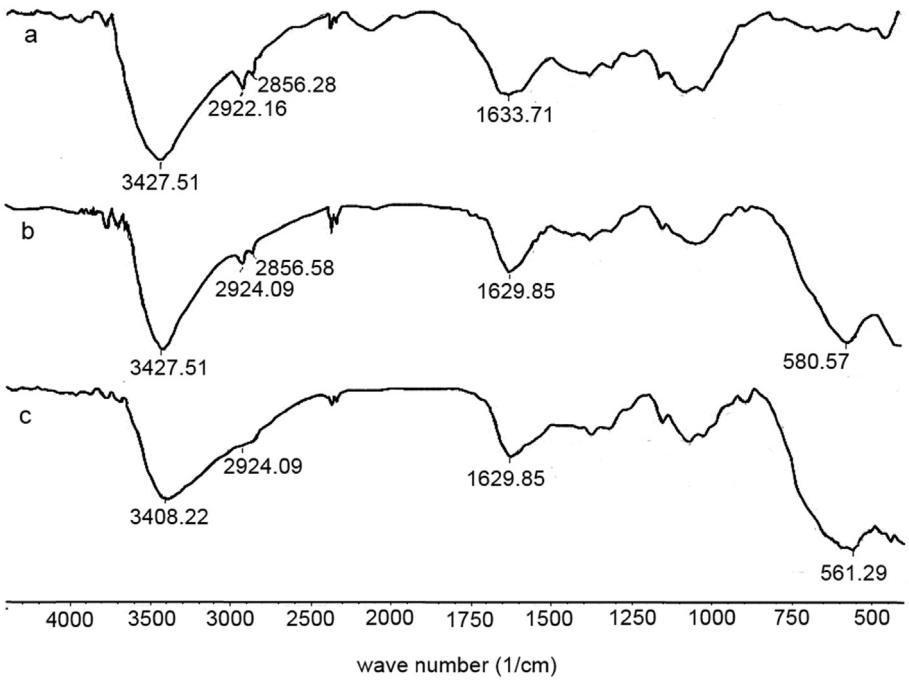

Fig. 1. FTIR spectra ofchitosan (a), magnetic chitosanwithout crosslinking (b) and magnetic chitosan with crosslinking (c).

shifted to 1629.85 cm^{-1}. It confirmed the formation of N=C between chitosan and glutaraldehyde [19]. Compared with Fig. 1(b), absorption band of Fe–O vibration at Fig. 1(c) appeared at lower wave number. It was probably due to the electrostatic force between Fe_3O_4 surface and glutaraldehyde. The absorption band of Fe–O still existed in the magnetic chitosan with crosslinking, which indicated Fe_3O_4 particles have been coated by crosslinked chitosan through the electrostatic interaction [20].

3.2. XRD

In this work, Fe_3O_4 was prepared from iron sand collected from Aceh, Indonesia. The XRD pattern of iron sand (Fig. 2b) showed typical pattern of Fe_3O_4 due to the main content of iron sand was Fe_3O_4.

Fig. 2c showed the XRD pattern of Fe_3O_4 isolated from iron sand, where it exhibited broad peaks at $2\theta = 35.42$ and 62.5° which were consistent with the standard pattern for JCPDS Card No. 89–4319 with lower peak intensities than iron sand. Low peak intensities confirmed the reduction of the crystallinity and particle size due to the isolation process. Sample that has a broad peak shows the nature and size of small crystals of a particle [21].

Diffractogram of chitosan exhibited typical peak of chitosan at $2\theta = 20^{o}$ (Fig. 2a). Diffractogram of magnetic chitosan with and without crosslinking (Fig. 2d and e) showed the loss of crystallinity of chitosan. It was due to glutaraldehyde immobilized chitosan chains. Therefore chitosan structure was less organized and caused more amorphous properties [18]. Amorphous structure of polymer leads high accessibility of Hg(II) to contact with active sites of chitosan during adsorption process. Typical peaks of Fe_3O_4 were also found in diffractogram of magnetic chitosan with and without crosslinking which confirmed the formation of the magnetic chitosan.

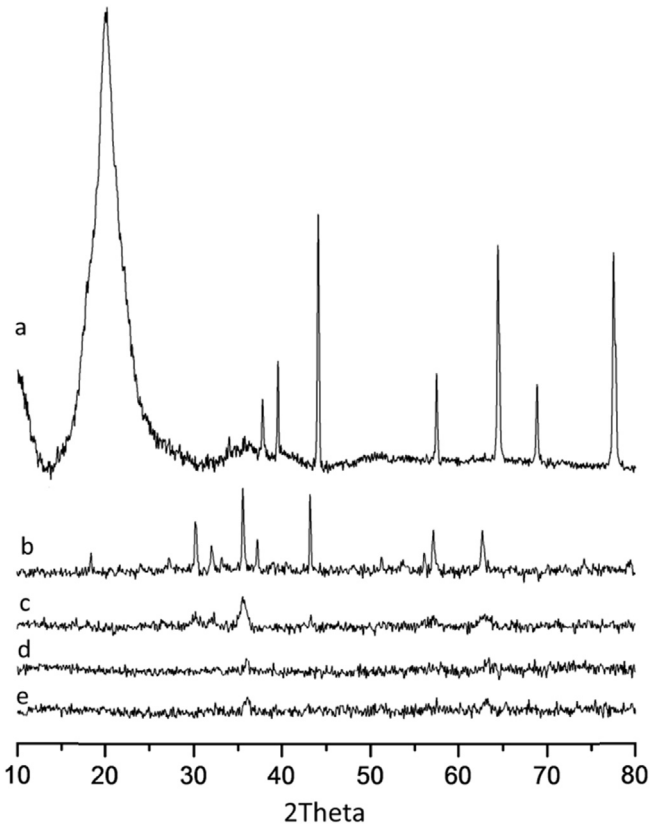

Fig. 2. XRD patterns of chitosan (a), iron sand (b), Fe_3O_4 isolated from iron sand (c) magnetic chitosan with crosslinking (d) magnetic chitosan without crosslinking (e).

3.3. SEM

SEM analysis was performed to study the morphology of the materials. Fig. 3 showed SEM images of iron sand, Fe_3O_4 isolated from iron sand, and magnetic chitosan with crosslinking. Based on SEM image of iron sand at magnification 500x, particle size of iron sand was about 125μm which larger than Fe_3O_4 isolated from iron sand. The structure of iron sand showed in SEM image at magnification 30,000x was as layered sheets (Fig. 3a). Nanosized particle of Fe_3O_4 was observed at magnification of 30,000x (Fig. 3b). These results indicated that Fe_3O_4 isolation from iron sand was successfully performed. The formation of nanosized Fe_3O_4 was also confirmed by XRD analysis. Nanosized particles of Fe_3O_4 formed aggregate become larger particle size as shown at magnification 500x. Fig. 3c was SEM image of magnetic chitosan with crosslinking. Magnetic chitosan showed rough surface. It was due to the addition of Fe_3O_4 as filler in crosslinked magnetic chitosan.

3.4. TGA/DSC

In order to study the thermal stability of chitosan and magnetic chitosan, TGA and DSC analysis were conducted. The results were shown in Fig. 4. Thermogravimetric curves of chitosan and magnetic chitosan were shown in Fig. 4a. Initial mass loss of both chitosan and magnetic chitosan was contributed to the moisture of samples. TGA curve of chitosan showed rapid weight drop from 300 °C to 380 °C resulting from decomposition of chitosan and there was no significant weight loss found above 380 °C. The weight loss behavior of magnetic chitosan was different from chitosan. Two main weight loss transitions were observed at 300–360 °C and 560–600 °C corresponding to the decomposition of chitosan and the reaction of Fe_3O_4 with carbon which was residue of the chitosan decomposition [22]. Fig. 4b showed endothermic peak at 115.67 °C in DSC curve chitosan and shifted to higher temperature in DSC curve of magnetic chitosan curve. It was due to the presence of Fe_3O_4 and crosslinking in the chitosan.

3.5. Adsorption studies

Initially, adsorption experiments were conducted to observe the influence of Fe_3O_4 particles and crosslinking agent addition on adsorption capacity of chitosan. The adsorption experiments were performed using chitosan alone, Fe_3O_4 particles alone and magnetic chitosan. The results show the adsorption capacity of chitosan alone and Fe_3O_4 alone were lower than magnetic chitosan (Fig. 5). After combination with Fe_3O_4 particles and crosslinking agent (glutaraldehyde), adsorption capacity of chitosan improved almost ten times compared than chitosan alone. It proves that this new material is potential to be used as an adsorbent of mercury.

3.5.1. Adsorption kinetics

Adsorption kinetics study is important because one of the criteria for efficiency of adsorbent is the rate of adsorption. In this work, the experiments were conducted with several contact times (0–100 min).

Fig. 6 showed adsorption capacity of Hg(II) by magnetic chitosan increased from initial time and tended to be constant after 80 min. The increase in adsorption capacity was due to the abundance of empty active sites of adsorbent. By increasing contact time, the active sites reduced and saturated at 80 min. The adsorption capacity was slightly decrease after 80 min due to the adsorption process was done under shaking that probably caused some adsorbed Hg(II) released from the surface of the adsorbent. However, the desorption of adsorbed Hg(II) was not significantly.

The pseudo first order and pseudo second order models were used to study adsorption kinetics of magnetic chitosan for Hg(II). The equations for pseudo first order and pseudo second order models were shown in Eqs. (2) and (3), respectively.

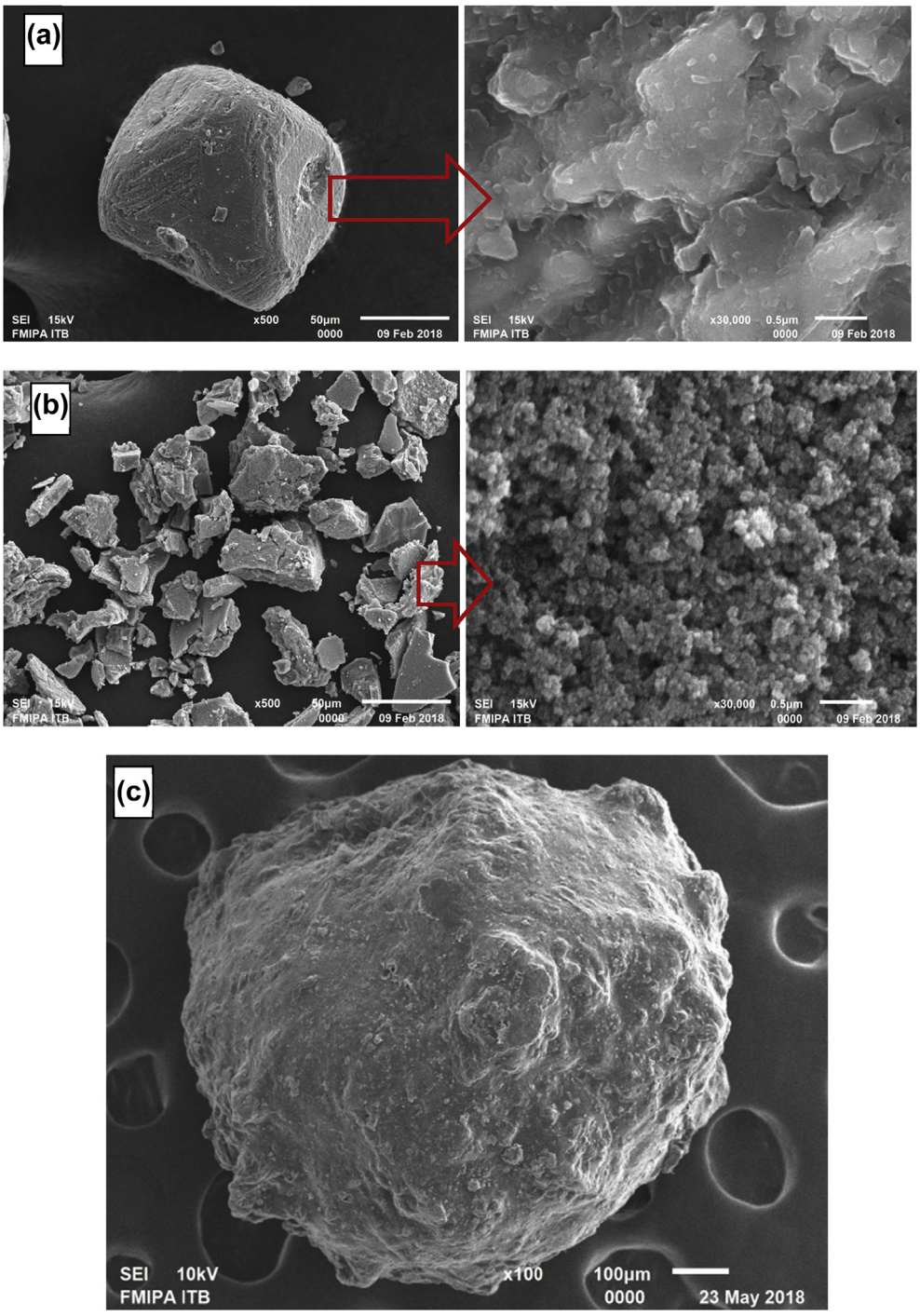

Fig. 3. SEM images of iron sand (a), Fe_3O_4 (b), and magnetic chitosan(c).

$$log\,(Q_e - Q_t) = \log Q_e - \frac{k_1}{2.303} \tag{2}$$

$$\frac{t}{Q_t} = \frac{1}{k_2 Q_e^2} + \frac{1}{Q_e}\,t \tag{3}$$

where Q_t and Q_e are the amount of solute adsorbed per mass of sorbent (adsorption capacity) at any time and equilibrium, respectively. k_1 is the rate constant of pseudo first order model and k_2 is the rate constant of pseudo second order model. Fitting data showed that the adsorption of Hg(II) by magnetic chitosan fitted to pseudo second order model (R^2 = 0.999; SSE = 0.655) (see Table 1).

3.5.2. *Influence of pH*

pH is one of very important factors in the overall adsorption process for heavy metal ions [23], particularly in adsorption capacity. Therefore in this work, the experiment was conducted with several pH values (2, 3, 4, 5, and 6). The adsorption processes were performed with initial concentration of Hg(II) 30 ppm for 80 min. The pH was adjusted by using 0.1 M NaOH and 0.1 M HCl. Fig. 7 showed an increase in adsorption capacity when the pH increased and tended to be constant after pH 4. At low pH, most of the active sites of chitosan will be protonated due to the abundance of H^+ in the solution. By increasing pH, H^+ content in the solution decreased resulting low competition between H^+ and Hg(II) ions to bind with active sites of chitosan and led the increase in adsorption capacity.

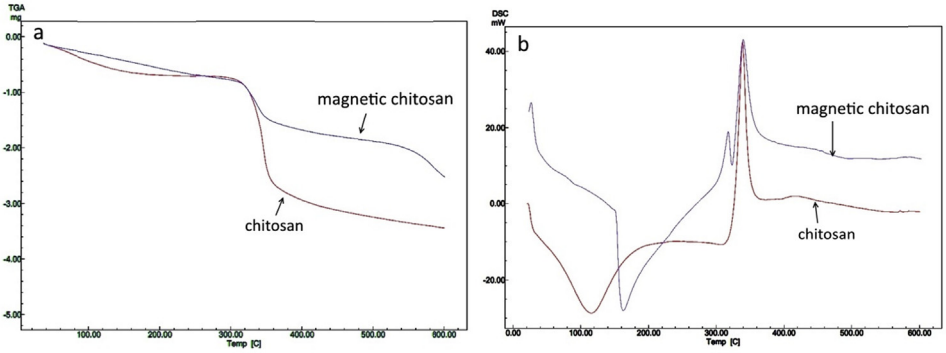

Fig. 4. TGA (a) and DSC (b) curves of chitosan and magnetic chitosan.

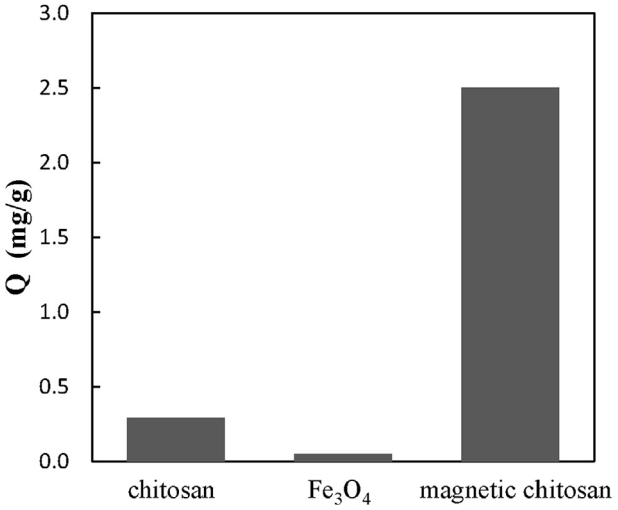

Fig. 5. Adsorption capacity of chitosan, Fe_3O_4 and magnetic chitosan for Hg(II) adsorption.

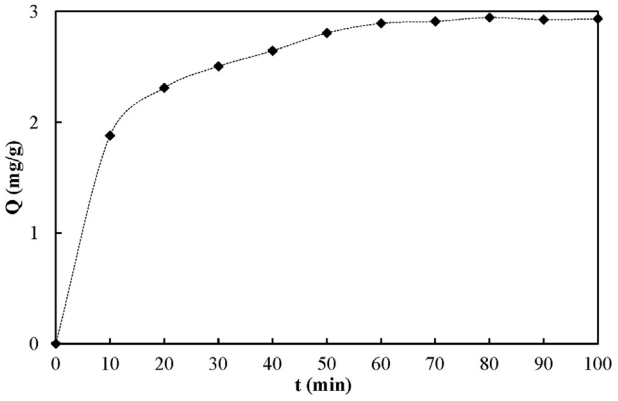

Fig. 6. Adsorption capacity of magnetic chitosan for Hg(II) adsorption at various contact times.

At higher pH, the adsorption capacity tended to be decreasing probably due to simultaneous adsorption and precipitation process.

3.5.3. Adsorption isotherms

The study of adsorption isotherms is essential for explaining the interaction between Hg(II) ions with an adsorbent. Adsorption isotherms in equilibrium condition describe the adsorbate distribution process between the liquid phase and the solid phase. In the adsorption isotherm, the process is illustrated by an equation or formula. The adsorption isotherms indicate the equilibrium relationship between the amount of metal ions adsorbed by the adsorbent. Langmuir adsorption isotherm model assumes monolayer adsorption and Freundlich adsorption isotherm model assumes multilayers adsorption. The equation of Langmuir and Freundlich adsorption isotherm models were shown in Eq. 4 and Eq. 5, respectively.

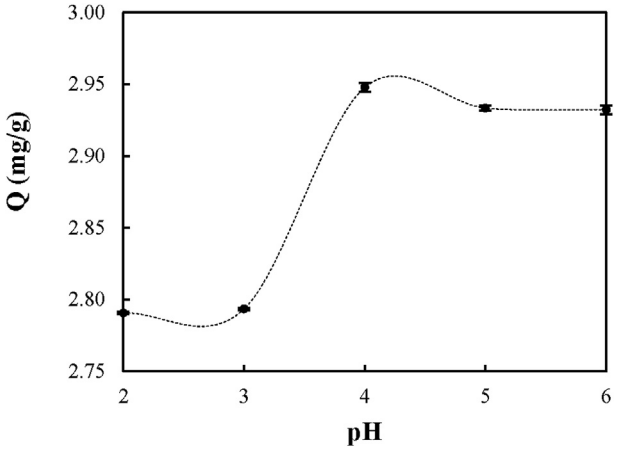

Fig. 7. Influence of pH on adsorption capacity of Hg(II) by magnetic chitosan.

$$Q_e = \frac{Q_m K_L C_e}{1 + K_L C_e} \quad (4)$$

$$Q_e = K_f C_e^{1/n} \quad (5)$$

In order to study the adsorption isotherm of magnetic chitosanfor Hg(II) adsorption, the adsorption experiments were conducted with several initial concentrations of Hg(II) (35, 40, 45, 50, 55, and 60 ppm) at pH 4 for 80 min. The results were shown in Fig. 8.

The best adsorption isoterm model for Hg(II) adsorption by magnetic chitosanwas determined based on R^2 and SSE values. Based on Table 2, both adsorption isotherm models showed $R^2 > 0.9$ that indicated the adsorption of Hg(II) by magnetic chitosan fitted to both models. However, SSE value of Langmuir adsorption isoterm model was lower than the SSE value of Freundlich adsorption isotherm model. It indicated that the adsorption process of Hg(II) by magnetic chitosan better fit to

Table 1
Kinetic parameters for Hg(II) adsorption by magnetic chitosan.

Pseudo first order				Pseudo second order			
R^2	Qe (mg/g)	k_1 (1/min)	SSE	R^2	Qe (mg/g)	k_2 (g/mg min)	SSE
0.898	2.204	0.057	0.699	0.999	3.178	0.047	0.655

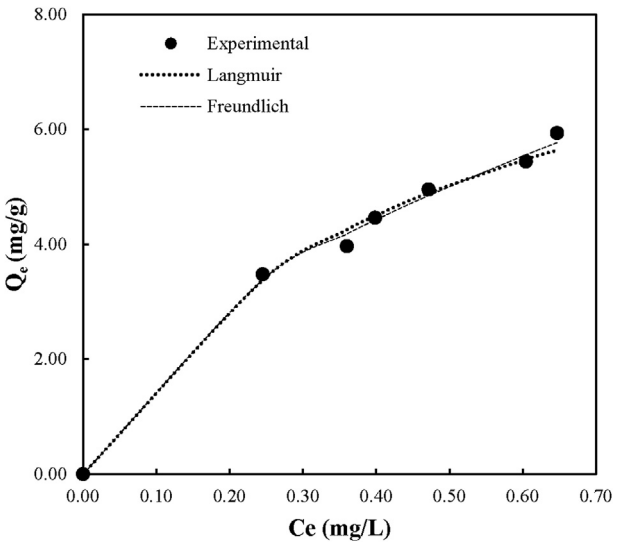

Fig. 8. Adsorption isotherm models of magnetic chitosanfor Hg(II) adsorption.

Table 2
Adsorption isotherm parameters for Hg(II) adsorption by magnetic chitosan.

Langmuir model				Freundlich model			
Q_m (mg/g)	K_L	R^2	SSE	K_f	n	R^2	SSE
9.53	2.24	0.95	0.0005	7.33	1.82	0.97	0.001

Q_m: maximum adsorption capacity; K_L: Langmuir constant; R^2: correlation coefficient; K_f:adsorption capacity; n: Freundlich constant; SSE: sum of square error.

Table 3
Maximum adsorption capacities of Hg(II) adsorption by some adsorbents.

Adsorbent	Q_m (mg/g)	Reference
Multiwalled carbon nanotubes	71.1 ± 7.3	[25]
Biomass of dried *Sargassumfusiforme*	30.86	[26]
Magnetic chitosan	9.53	This work
Powdered swamp arum *(Lasimorphasenegalensis)* seeds.	5.917	[27]
Water hyacinth roots	5.53	[28]
Spherical activated carbons	3.580	[29]
Peanut shells	1.90	[30]
Garlic (*Allium sativum* L.) powder	0.6497	[31]
Glutaraldehyde cross-linked chitosan	0.0077	[32]

Langmuir than Freundlich adsorption isotherm models. Based on Langmuir adsorption isotherm model, the maximum adsorption capacity (Q_m) obtained in this work was 9.53 mg/g. The comparison of the maximum adsorption capacity of Hg(II) adsorption by some adsorbents was shown in Table 3.

The relative ability of adsorbent in adsorption of adsorbate can be determined by using the value of K_f. The strength of the interaction between adsorbent and adsorbatecan be expressed by n value. If $n < 1$, the adsorption process is physical adsorption. If $n > 1$, the adsorption is chemical adsorption [24]. The values of K_f and n for adsorption Hg(II) by magnetic chitosanwere 7.33 and 1.82, respectively. It indicated the adsorption processes is chemical adsorption. Chemical adsorption occurs when chemical bonds are formed between dissolved substances in solution with adsorbent. In the case of adsorption Hg(II) by crosslinked magnetic chitosan composite beads, the adsorption occur due to the formation of chelate between amino groups of chitosan and Hg(II) ion. Another possibility was electrostatic force between $Fe_3O_4$and Hg(II).

In order to confirm the adsorption capacity of magnetic chitosan on Hg(II) adsorption, the quantification of elemental composition before and after adsorption were performed using EDS and the results were shown in Fig. 9. The results show mercury was not found in the magnetic chitosan before adsorption. After adsorption, mercury was observed in the magnetic chitosan. Based on weight percentage of mercury in the adsorbent (1.482%), the adsorption capacity of mercury by magnetic chitosan was 15.04 mg/g. Compared with some adsorbents in Table 3, the magnetic chitosan shows relatively higher adsorption capacity.

3.5.4. *Recycling study*

Chitosan magnetic was recycled using HNO_3 0.001 N, where recycle process was began with the desorption of adsorbed Hg(II) on the used magnetic chitosan. The magnetic chitosan was then separated from the solution and washed with distilled water until neutral pH was reached. The magnetic chitosan was dried and reused as an adsorbent. The results were shown in Fig. 10.

In the first recycle, chitosan magnetic showed the highest adsorption capacity. In the subsequent recycles, the adsorption capacity of magnetic chitosan decreased. However, the decrease was not significantly. The decrease was due to the adsorbed Hg(II) could not be removed totally. It still bind with active sites of the adsorbent that prevented Hg(II) in the solution to bind with the adsorbent. The amounts of mercury in the magnetic chitosan after 1st, 2nd, 3rd, and 4th wash were 0.177, 0.180, 0.280, and 1.059% (weight %), respectively. The chitosan magnetic

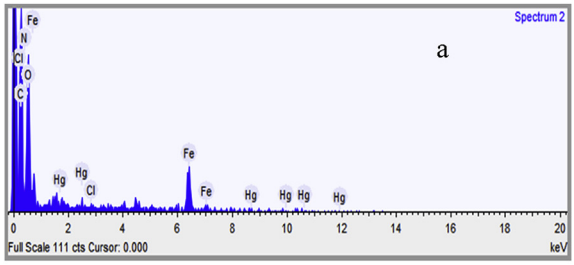

Element	Weight %	Weight % σ	Atomic %
Carbon	36.158	4.284	47.009
Nitrogen	6.755	7.781	7.531
Oxygen	42.329	4.447	41.315
Chlorine	0.115	0.190	0.051
Iron	14.643	1.847	4.094
Mercury	0.000	0.000	0.000

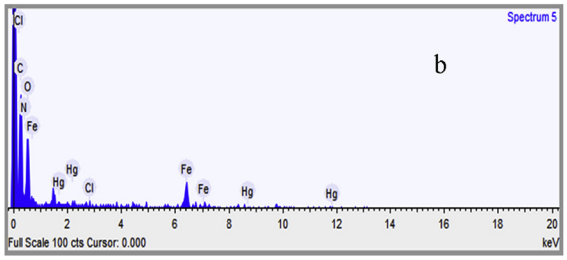

Element	Weight %	Weight % σ	Atomic %
Carbon	30.523	4.305	39.480
Nitrogen	18.112	6.375	20.088
Oxygen	38.131	4.291	37.026
Chlorine	0.133	0.207	0.058
Iron	11.620	1.743	3.232
Mercury	1.482	0.702	0.115

Fig. 9. EDS analysis of magnetic chitosan before (a) and after (b) adsorption.

particles can be recycled for four times and they become collapse after fourth recycle. This suggests that magnetic chitosan is recyclable and reused as an adsorbent repeatedly.

3.5.5. Application of magnetic chitosan for removal mercury from real polluted water

Some traditional gold mining processes in Aceh, Indonesia polluted the environment by mercury that harmful for the aquatic system. It was due to the wastewater of gold mining process was directly discharged into the aquatic environment without processing. The high level of mercury in the aquatic environment causes anxiety and adverse effects on living organisms in these waters, even endanger human health that use water and consume the organisms contained in the water. Therefore, themagnetic chitosan obtained in this work was applied as an adsorbent of mercury from polluted water in river close to gold mining area at Manggamat, Aceh, Indonesia. The samples were collected for every 50 m along river close to gold mining area. The mercury concentrations of some polluted water before and after adsorption were determined by using AAS. The removal percentage (R) was calculated using Eq. (6).

$$R\,(\%) = \frac{(C_i - C_e)}{C_i} \times 100 \quad (6)$$

Table 4 showed general analysis of polluted water. After adsorption processes by using magnetic chitosan, the mercury concentrations were decreased with various removal percentages (Fig. 11). The difference of removal percentage was probably due to the different components content of the polluted water (Table 4). The polluted water at sampling point 4 showed the highest salinity than other sampling points. It also contained the largest amount of Fe ions among six sampling points. The existence of others ions in the polluted water will reduce adsorption capacity due to the competition of Hg with other ions to bind with active sites. Therefore, polluted water at sampling point 4 showed the lowest removal percentage. The highest removal percentage was obtained at sampling point 6 (96.13%)

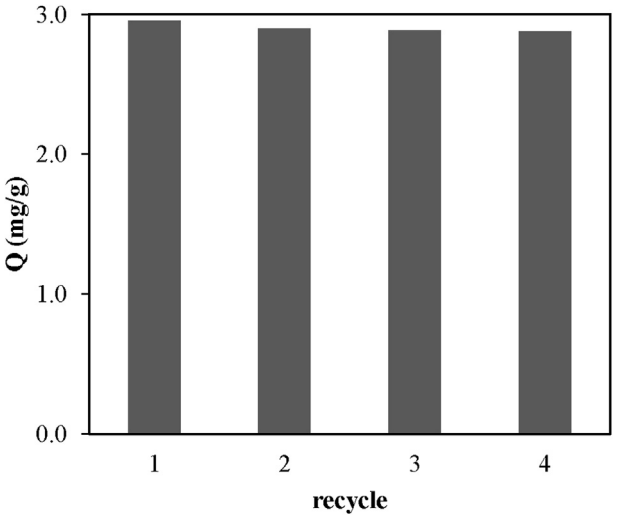

Fig. 10. Adsorption capacity of Hg(II) by magnetic chitosan after recycle.

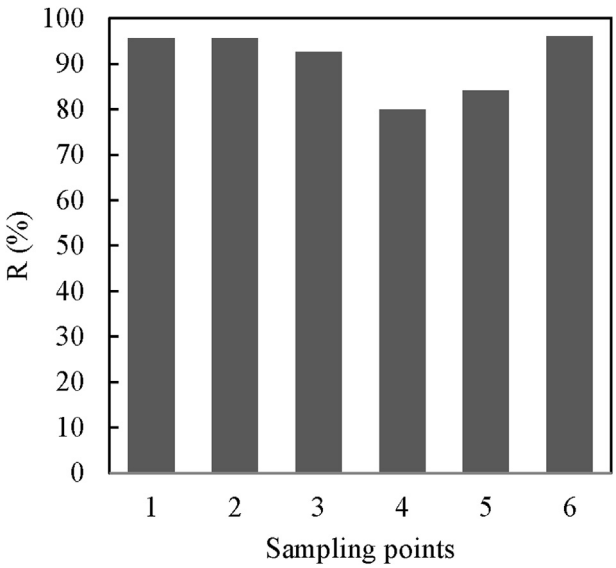

Fig. 11. Magnetic chitosan treated polluted water.

4. Conclusions

Fe_3O_4 isolated from iron sand had been obtained and used in magnetic chitosan preparation. Magnetic chitosan produced was confirmed by FTIR, TGA, DSC, XRD and SEM analysis. Fe_3O_4 and glutaraldehyde loading in chitosan composite beads decreased crystallinity of chitosan. Low crystallinity is favorable for adsorption due to high accessibility of adsorbate to bind with active sites of adsorbent. Adsorption study showed magnetic chitosan could be effectively used for Hg(II) removal from polluted water. Hg(II) adsorption by magnetic chitosanwas fit to Langmuir and Freundlich isotherm models. Removal percentage of mercury removal from real polluted water by magnetic chitosan reached 96.13%. In conclusion, results obtained suggest that magnetic chitosan has a high potential as an adsorbent of mercury in polluted water.

Declarations

Author contribution statement

Rahmi: Conceived and designed the experiments; Performed the experiments; Analyzed and interpreted the data; Contributed reagents, materials, analysis tools or data; Wrote the paper.

Fathurrahmi, Fitri Purnama Wati: Performed the experiments.

Lelifajri: Analyzed and interpreted the data.

Table 4
General analysis of polluted water.

Sampling point	pH	TDS	Salinity	Ions (mg/L)					
		(mg/L)	(ppt)	Hg	Cd	Fe	Pb	Cu	Mn
1	8.31	15,300	17.4	0.110	0.0368	<0.009	ND	0.1010	<0.002
2	8.36	11,200	13.4	0.110	0.0391	0.1083	ND	0.1060	<0.002
3	8.44	7,400	11.4	0.116	0.0435	0.0644	ND	0.3469	<0.002
4	8.32	14,000	18.1	0.061	0.0469	2.7106	ND	0.0918	<0.002
5	8.34	13,200	16.4	0.119	0.0474	1.7358	ND	0.1373	<0.002
6	8.47	10,000	12.6	0.362	0.0385	<0.009	1.1815	0.0463	<0.002

ND:not detected.

Funding statement

This work was supported by Direktorat Riset dan Pengabdian Masyarakat, Direktorat Jenderal Penguatan Riset dan Pengembangan Kementerian Riset, Teknologi, dan Pendidikan Tinggi Republik Indonesia (grant number 04/UN11.2/PP/SP3/2018).

Competing interest statement

The authors declare no conflict of interest.

Additional information

No additional information is available for this paper.

References

[1] Q. Wang, D. Kim, D.D. Dionysiou, G.A. Sorial, D. Timberlake, Sources and remediation for mercury contamination in aquatic system- a literature review, Environ. Pollut. 131 (2004) 323–336.
[2] A. Kudo, S. Miyahara, A case history: minamata mercury pollution in Japan-from loss of human lives to decontamination, Water Sci. Technol. 23 (1991) 283–290.
[3] L. Daza, S. Mendioroz, J.A. Pajares, Mercury adsorption by sulfurized fibrous silicates, Clay Clay Miner. 39 (1) (1991) 14–21.
[4] D. Sarkar, M.E. Essington, K.C. Misra, Adsorption of mercury(II) by variable charge surfaces of quartz and gibbsite, Soil Sci. Soc. Am. J. 63 (1999) 1626–1636.
[5] L. Pulido-Novicio, Y. Kurimoto, M. Aoyama, K. Seki, S. Doi, T. Hata, S. Ishihara, Y. Imamura, Adsorption of mercury by sugi wood carbonized at 1000°C, J. Wood Sci. 47 (2001) 159–162.
[6] M. Wan, C. Kan, B.D. Rogel, M.L.P. Dalida, Adsorption of copper (II) and lead (II) ions from aqueous solution on chitosan-coated sand, Carbohydr. Polym. 80 (9) (2010) 891–899.
[7] S. De Gisi, G. Lofrano, M. Grassi, M. Notarnicola, Characteristics and adsorption capacities of low-cost sorbents for wastewater treatment: a review, Sustainable Materials and Technologies 9 (2016) 10–40.
[8] C. Jeon, W.H. Holl, Chemical modification of chitosan and equilibrium study for mercury ion removal, Water Res. 37 (2003) 4770–4780.
[9] W.S.W. Ngah, L.C. Teong, M.A.K.M. Hanafiah, Adsorption of dyes and heavy metal ions by chitosan composite beadss: a review, Carbohydr. Polym. 83 (2011) 1446–1456.
[10] F. Allouche, E. Guibal, N. Mameri, Preparation of a new chitosan-based material and its application for mercury sorption, Colloid. Surf. Physicochem. Eng. Asp. 446 (2014) 224–232.
[11] U. Habiba, T.A. Siddique, J.J.L. Lee, T.C. Joo, A.M. Afifi, B.C. Ang, Adsorption study of methyl orange by chitosan/polyvinyl alcohol/zeolite electrospuncomposite beadsnanofibrous membrane, Carbohydr. Polym. 191 (2018) 79–85.
[12] L. Zhou, Z. Liu, J. Liu, Q. Huang, Adsorption of Hg(II) from aqueous solution by ethylenediamine-modified magnetic crosslinking chitosan microspheres, Desalination 258 (2010) 41–47.
[13] A.T. Paulino, L.A. Belfiore, L.T. Kubota, E.C. Muniz, Almeida, E.B. Tambourgi, Effect of magnetite on the adsorption behavior V. C., of Pb(II), Cd(II), and Cu(II) in chitosan-based hydrogels, Desalination 275 (2011) 187–196.
[14] C. Fan, K. Li, Y. He, Y. Wang, X. Qian, J. Jia, Evaluation of magnetic chitosan composite beads beads for adsorption of heavy metal ions, Sci. Total Environ. 627 (2018) 1396–1403.
[15] I.A. Udoetok, L.D. Wilson, J.V. Headley, Self-assembled and cross-linked animal and plant-based polysaccharides: chitosan–cellulose composites and their anion uptake properties, ACS Appl. Mater. Interfaces 8 (2016) 33197–33209.
[16] H. Judawisastra, L.O.C. Hadyiswanto, W. Winiati, The effect of demineralization process on diameter, tensile properties and biodegradation of chitosan fiber, Procedia Chem. 4 (8) (2012) 138–145.
[17] S. Asgari, Z. Fakhari, S. Berijani, Syinthesis and characterization of Fe_3O_4 magnetic nanoparticles coated with carboxymethil chitosan grafted sodium methacrylate, J. Nanostruct. 4 (2014) 55–63.
[18] Y. Ding, S.Z. Shen, H. Sun, K. Sun, F. Liu, Y. Qi, J. Yan, Design and construction of polymerized-chitosan coated Fe_3O_4 magnetic nanoparticles and its application for hydrophobic drug delivery, J. Mater. Sci. Eng. 48 (2014) 487–498.
[19] M.M. Beppu, R.S. Vieira, C.G. Aimoli, C.C. Santana, Crosslinking of chitosan membranes using glutaraldehyde: effect on ion permeability and water adsorption, J. Membr. Sci. 301 (2007) 126–130.
[20] G. Li, Y. Jiang, K. Huang, P. Ding, J. Chen, Preparation and properties of magnetic Fe_3O_4–chitosan nanoparticles, J. Alloy. Comp. 466 (2008) 451–456.
[21] T. Saranya, K. Parasuraman, M. Anbarasu, K. Balamurugan, XRD, FT-IR, and SEM study of magnetite (Fe_3O_4) nanoparticles prepared by hydrothermal method, Nano Vision 5 (2015) 4–6.
[22] H. Ma, S. Pu, Y. Hou, R. Zhu, A. Zinchenko, W. Chu, A highly efficient magnetic chitosan "fluid" adsorbent with high capacity and fast adsorption kinetics for dyeing wastewaer purification, Chem. Eng. J. 345 (2018) 556–565.
[23] M. Monier, D.A. Abdel-Latif, Modification and characterization of PET fibers for fast removal of Hg(II), Cu(II) and Co(II) metal ions from aqueous solutions, J. Hazard Mater. 250– 251 (2013) 122–130.
[24] W.L. Chou, C.T. Wang, W.C. Chang, S.Y. Chang, Adsorption treatment of oxide chemical mechanical polishing wastewater from a semiconductor manufacturing plant by electrocoagulation, J. Hazard Mater. 180 (2010) 217–224.
[25] D. Zhang, Y. Yin, J. Liu, Removal of Hg^{2+} and methyl mercury in waters by functionalized multi-walled carbon nanotubes: adsorption behavior and the impacts of some environmentally relevant factors, Chem. Speciat. Bioavailab. 29 (1) (2017) 161–169.
[26] S. Huang, G. Lin, Biosorption of Hg(II) and Cu(II) by biomass of dried Sargassumfusiforme in aquatic solution, Journal of Environmental Health Science & Engineering 13 (21) (2015) 1–8.
[27] T. Tarawou, Y. Erepamowel, Equilibrium sorption studies of Hg (II) ions from aqueous solution using powdered swamp arum *(Lasimorphasenegalensis)* seeds, J. Appl. Sci. Environ. Manag. 20 (2) (2016) 221–225.
[28] G. Padmapriya, A.G. Murugesan, Biosorption of Hg(II) ions from aqueous solution using the aquatic weed water hyacinth with equilibrium and kinetic modeling, Remediation 23 (2) (2013) 127–139.
[29] W. Chen, Kinetic modeling on the adsorption of vapor-phase mercury chloride on activated carbon by thermogravimetric analysis, J. Air Waste Manag. Assoc. 59 (2) (2009) 227–235.
[30] Y. Liu, X. Sun, B. Li, Adsorption of Hg^{2+} and Cd^{2+} by ethylenediamine modified peanut shells, Carbohydr. Polym. 81 (2) (2010) 335–339.
[31] Y. Eom, J.H. Won, J. Ryu, T.G. Lee, Biosorption of mercury(II) ions from aqueous solution by garlic (*Allium sativum* L.) powder, Korean J. Chem. Eng. 28 (6) (2011) 1439–1443.
[32] S. Kushwaha, P.P. Sudhakar, Adsorption of mercury(II), methyl mercury(II) and phenyl mercury(II) on chitosan cross-linked with a barbital derivative, Carbohydr. Polym. 86 (2) (2011) 1055–1062.